TOWARDS ACCURATE, HIGH-FREQUENCY I-V CURVE MEASUREMENTS OF PHOTOVOLTAIC MODULES APPLYING ELECTRONIC LOADS

K. Spiliotis[1,2,4], G.H. Yordanov[1,2], G. Van den Broeck[1,2,4], H. Goverde[2,3], K. Baert[1,2], J. Driesen[1,2]

[1]KU Leuven, ESAT-ELECTA, Kasteelpark Arenberg 10, 3001 Leuven-Heverlee, Belgium
[2]EnergyVille, ThorPark 8310, 3600 Genk, Belgium
[3]IMEC, Kapeldref 75, 3001, Leuven-Heverlee, Belgium
[4]EIT InnoEnergy, J.F. Kennedylaan 2, 5612 AB Eindhoven, The Netherlands

ABSTRACT: We present a new measurement methodology for accurate, high-frequency outdoor I-V characterization of PV modules. A hybrid sweep is performed in order to obtain more detailed I-V curves of the PV module, hereby combining the advantage of a voltage sweep (for good resolution in the near-horizontal parts of the curve) with the advantage of a current sweep (giving precise information about the very steep parts). The new approach is compared to the state-of-the-art current and voltage sweep methods. Furthermore, an advanced data-point distribution algorithm is discussed, which ensures sufficient information in the ranges of interest, while keeping the total amount of required measurement points as low as possible to minimize the data storage, sweep time, and computational effort. The improved technique provides accurate, high-resolution characterization about the maximum power point, MPP without necessarily requiring too many measurement points. The new methods enable I-V measurement frequencies up to 1 Hz (which is essential for accurate energy yield estimations) while maintaining low computational effort.

Keywords: PV Module, Electrical characterization, Hybrid I-V sweep, Measurement automation.

1 INTRODUCTION

An important part of the PV modules development at EnergyVille is the outdoor performance testing. To be able to estimate and model the energy yield also during highly varying weather conditions, high frequency (1 Hz) and accurate I-V characterization is required [1]. However, at this sampling rate, the amount of data produced can be enormous, hereby strongly enlarging the storage demand and limiting data processing capabilities due to a big computational effort required to lookup the measured data. Next to that, state-of-the-art current and voltage sweeping methods produce detailed information between the MPP and open circuit voltage as well as from short circuit current up to the MPP, respectively. Accurate and detailed information about the complete IV curve is required for analyses of both the degradation and the energy production.

2 STATE OF THE ART

The I-V curves of PV modules provide valuable information for their performance, such as the values of short-circuit current (**I_{SC}**), open-circuit voltage (**V_{OC}**) and the MPP location. Common ways to sweep the I-V curve include the use of variable resistor [2, 3], capacitive load [4], electronic load [5-7], bipolar power amplifier [8], four-quadrant power supply [9], and DC-DC converters [10]. Multichannel electronic loads are characterized by high degree of flexibility and modularity [11]. That makes them well suited for technical and scientific research. Some experimental setups use electronic loads for I-V curve estimation and MPP tracking [12-14]. Electronic loads are based on MOSFETs and use current or voltage ramps in order to sweep the I-V curve of the connected PV module. Non-monotonic voltage control waveforms are used to measure accurate I-V curves of highly capacitive PV modules with short-pulse (~10 ms) sun simulators. Studies concerning energy yield, ageing, control and balancing among others require accurate I-V characteristics to ensure reliable results. Often, the means of improving the I-V curve measurement is by increasing the number of set points, decreasing the stepping time and dynamically estimating their distribution. These approaches, however, come along with certain drawbacks. An increased number of set points results in high volumes of data; dynamic measurement point setting requires continuous and fast computations; while decreased time intervals between I-V point measurements require costly high-performance load controllers or prolonged operation away from the MPP which results in higher operating temperatures of the PV cells.

3 METHODOLOGY AND NOVEL APPROACHES

As part of an outdoor measurement campaign for testing innovative façade BIPV modules, KU Leuven and IMEC carry out experiments involving 9-cell c-Si modules without bypass diodes [13-15]. Within this campaign, the present work proposes two new approaches for I-V curve sweeping developed in such a way as to avoid the aforementioned complications. A voltage-controlled sweep would obtain more information on the flat part of the I-V curve, while a current-controlled sweep emphasizes the rest. The proposed approaches are designed to obtain high detail on the entire I-V without extra computing cost. They have been conceptualized and implemented experimentally.

3.1 Variable-step current sweep

The I-V curve measurement specification requires **N** = 50 data points per curve, each being an average of 20 voltage and current measurements. Because of the good quality cells used in the modules, the shunt resistance is very high and the lack of bypass diodes results in I-V curves that are very flat between short circuit and the kink near the maximum power point (MPP); see Fig. 1. Kinks result when one cell limits the current output of the entire string, which results in a cut-off. Often the MPP is located at the kink, meaning that the associated P-V curve is not differentiable at this point. Therefore, a very good resolution is mandatory for achieving low uncertainties of the power, current and voltage at the MPP.

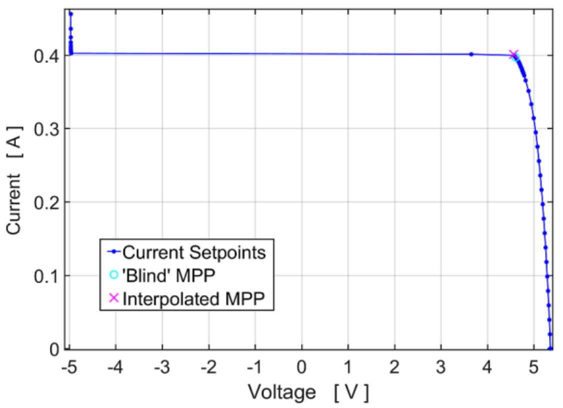

Figure 1: I-V curve of a 9-cell c-Si PV module without bypass diodes measured with the described in section 3.1

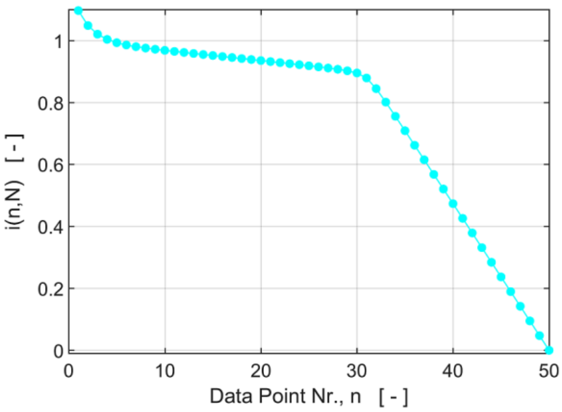

Figure 2: The current setpoints function $\boldsymbol{i}(\mathbf{n},\mathbf{N})$ calculated for $\mathbf{N}$ = 50 data points per I-V curve according to the method described in section 3.1.

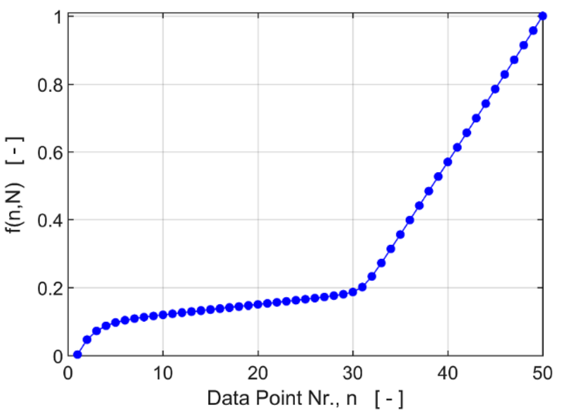

Figure 3: The auxiliary function $\boldsymbol{f}(\mathbf{n},\mathbf{N})$ calculated for $\mathbf{N}$ = 50 data points per I-V curve.

Because of the low number of data points being recorded for each I-V curve, we had to distribute these points optimally so that the best resolution is achieved about the MPP. For c-Si PV cells and modules, the latter is usually achieved between 92% and 95% of the short-circuit current, $\mathbf{I}_{SC}$ [16]. However, when there is a cut-off due to a cell that significantly underperforms the others, the MPP may be at the kink and the $\mathbf{I}_{MPP}$ is almost equal to the $\mathbf{I}_{SC}$. Therefore, we aimed for best resolution (densest data points) between about 0.90$\mathbf{I}_{SC}$ and 1.00$\mathbf{I}_{SC}$. The short-circuit current is measured before the I-V curve. Then, we define the current setpoints for the electronic load control between 1.10$\mathbf{I}_{SC}$ and 0 A in case the in-plane solar irradiance increases in the meantime. This particular multichannel electronic load is operated in constant current mode because all the other modes require unacceptably long measurement times for a complete I-V curve.

We need a scalable solution that works for an arbitrary, but not too low, number of data points per I-V curve, $\mathbf{N} \geq 50$. For a given $\mathbf{N}$, our data-acquisition (DAQ) software calculates a vector of $\mathbf{N}$ elements containing the desired setpoints in terms of parts of the $\mathbf{I}_{SC}$; see Figure 2. The current setpoints are then obtained by multiplying that vector by the measured $\mathbf{I}_{SC}$. To obtain these optimal values along the I-V curve, we take the following approach. We define a dimensionless function $\boldsymbol{i}(\mathbf{n},\mathbf{N}) = 1.10(1 - \boldsymbol{f}(\mathbf{n},\mathbf{N}))$ where $\mathbf{n}$ is the data point number ($\mathbf{n}$ = 1 corresponding to 110% of $\mathbf{I}_{SC}$ and $\mathbf{n} = \mathbf{N}$ corresponding to open circuit) while $\boldsymbol{f}(\mathbf{n},\mathbf{N})$ is an auxiliary function (also dimensionless) which satisfies $\boldsymbol{f}(1,\mathbf{N}) = 0$ and $\boldsymbol{f}(\mathbf{N},\mathbf{N}) = 1.00$. Examples for $\boldsymbol{i}(\mathbf{n},\mathbf{N})$ and $\boldsymbol{f}(\mathbf{n},\mathbf{N})$ are given in Figs. 2 and 3, respectively for $\mathbf{N}$ = 50. We model the auxiliary function $\boldsymbol{f}(\mathbf{n},\mathbf{N})$ as a hyperbola which undergoes translation and rotation with respect to the origin of the coordinate system, and subtract an exponentially decaying term to obtain the required curving at the low $\mathbf{n}$ values. We require that, independent on $\mathbf{N}$, approximately a tenth of all the data points in the I-V curve lie between 1.10$\mathbf{I}_{SC}$ and 1.00$\mathbf{I}_{SC}$; half of all points lie between 1.00$\mathbf{I}_{SC}$ and 0.90$\mathbf{I}_{SC}$; and the rest are more or less evenly distributed from 0.90$\mathbf{I}_{SC}$ down to open circuit ($\mathbf{I}$ = 0 A). We use these requirements to parameterize the hyperbolic and exponential parts of the auxiliary function $\boldsymbol{f}(\mathbf{n},\mathbf{N})$ as well as the initial translation and rotation of the hyperbola. For brevity, the involved equations are omitted in the present paper. With this approach, we obtain satisfactory resolution of the measured I-V curves and P_{max} accuracy within 0.6%. Fig. 1 shows an example 2-quadrant I-V curve for one of the tested modules. The circle and the cross represent the MPP location as determined from the original and fitted curve, respectively.

3.2 Hybrid sweep

A hybrid sweeping scheme is employed, where two sweeps are performed (in voltage and current control mode) to emphasize different parts of the I-V curve. The voltage sweep gives enough points in flat near-horizontal regions, while the current sweep does so in near-vertical parts. Specifically, the method includes a current sweep with k equidistant current set points between 0 A and 92%-95% of $\mathbf{I}_{SC}$ [16], followed by equidistant voltage set points starting from 0 V and increasing to $\mathbf{V}_{OC}$. We can see in Fig. 4 an illustration of the proposed sweep strategy. We can clearly observe that in case of a current sweep for example, the resolution of our current set points has to be drastically increased close to $\mathbf{I}_{SC}$ or the local level of detail will suffer. Similarly, much finer voltage steps would be required between $\mathbf{V}_{k}$ and $\mathbf{V}_{OC}$. Sweeping between 0 A and $\mathbf{I}_{SC}$ and 0 V and $\mathbf{V}_{OC}$, with few equidistant current and voltage set points accordingly may provide accurate enough I-V characteristic without increasing the number of data points. $\mathbf{I}_{MPP}$ and $\mathbf{V}_{MPP}$ are approximated through $\mathbf{I}_{k}$ and $\mathbf{V}_{k}$, respectively. I-V curves of partially shaded modules with bypass diodes require complete current and voltage sweeps since the MPP location is generally unknown a priori. Partially shaded modules with integral bypass diodes in each cell (e.g. with SunPower Maxeon Gen III IBC cells) require many more data points for greater detail. Fig. 5 depicts our proposed hybrid I-V curve sweeping algorithm.

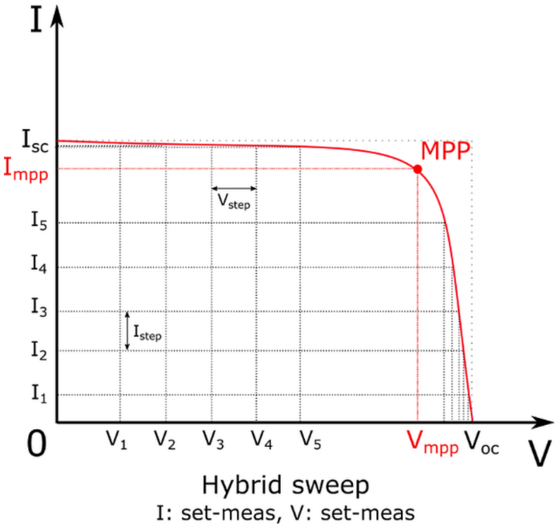

Figure 4: Hybrid sweeping on the I-V curve.

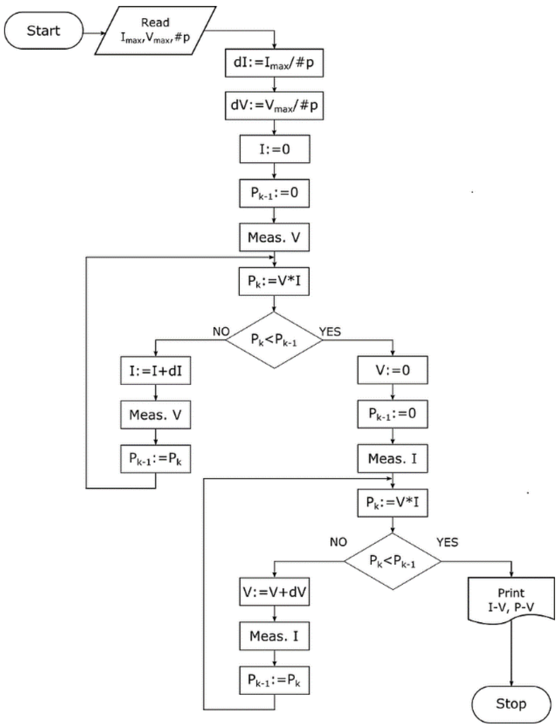

Figure 5: Flowchart depicting the hybrid sweeping algorithm.

4 RESULTS AND DISCUSSION

The voltage and current sweeps alongside the novel methodology are implemented in practice using 9-cell c-Si PV modules without bypass diodes, Höckerl & Hackl PMLI and PLI-606 electronic loads, and National Instruments compactRIO and compactDAQ controllers programmed with LabVIEW-based software.

Figs. 6 and 7 and illustrate the performance of the hybrid sweep compared to the voltage and current sweeps for a certain number of measurement points. Specifically, the sweeps' performance is tested using between 50 and 300 measurement points. We see that with a hybrid sweep even as few as 50 points may suffice to determine the **MPP**, $\mathbf{I_{SC}}$, and $\mathbf{V_{OC}}$. It is clear that, at a low number of data points, the region close to $\mathbf{V_{OC}}$ cannot be resolved satisfactory when performing an equidistant voltage sweep. Similarly, the flat part of the I-V curve needs to be interpolated when applying a current sweep. Hybrid sweeping may help to estimate more accurately the series and shunt resistance, $\mathbf{R_S}$ and $\mathbf{R_P}$, as it provides a lot of information about the flat parts of the curve.

Fig. 8 shows P-V curves of seven BIPV modules in the MPP vicinity. The corresponding I-V curves were obtained with the variable-step current sweep algorithm. Although the optimal data point density is not always achieved at the MPP, the finer steps around it allows for accurate curvilinear fitting for MPP interpolation.

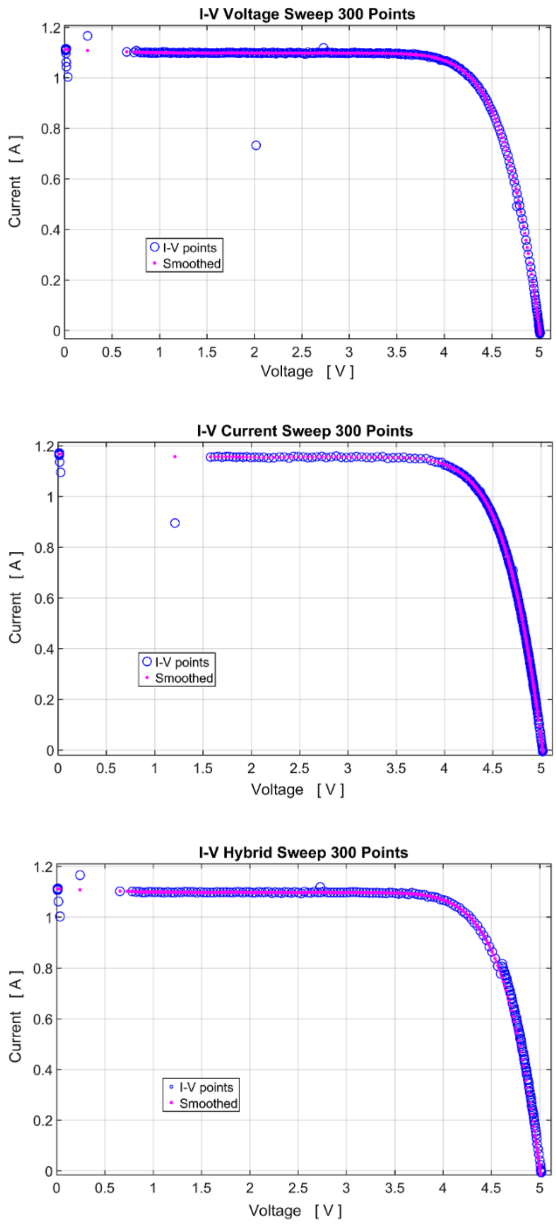

Figure 6: Voltage, current and hybrid sweeping (from top to bottom) for 300 data points.

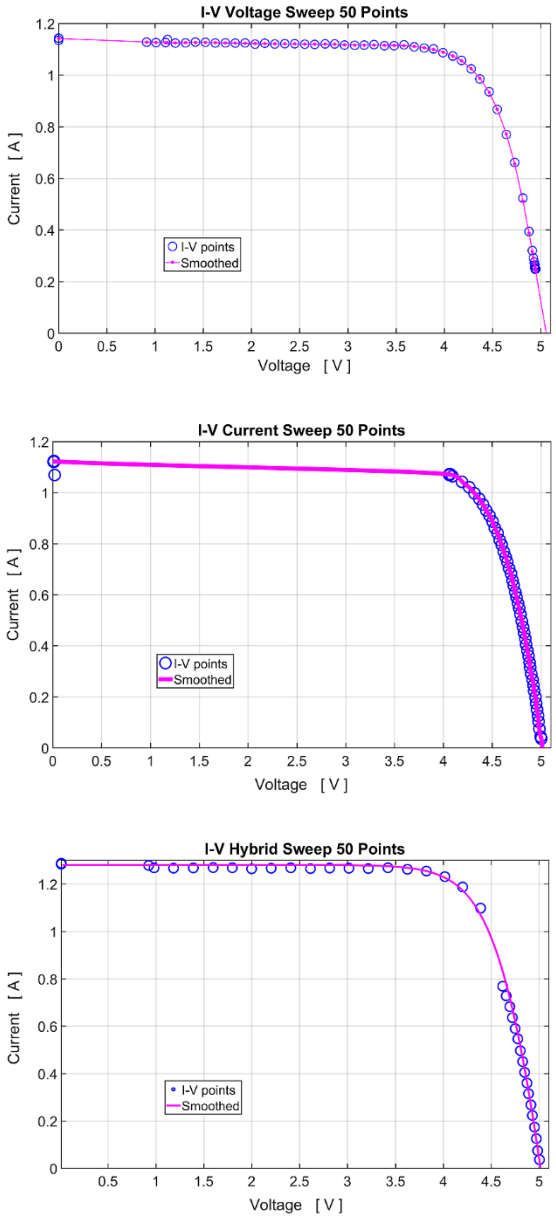

Figure 7: Voltage, current and hybrid sweep (from top to bottom) for 50 data points

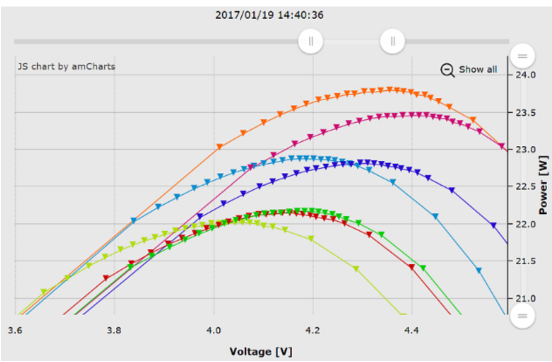

Figure 8: A screenshot from the data-querying web interface showing P-V curves of seven BIPV minimodules near the MPPs.

Finally, Fig. 9 shows results from simulated hybrid sweep of a stepped I-V curve of a 60-cell c-Si PV module with three bypass diodes and different degree of shading in the three sub-strings. The simulations were done in Matlab using Simulink.

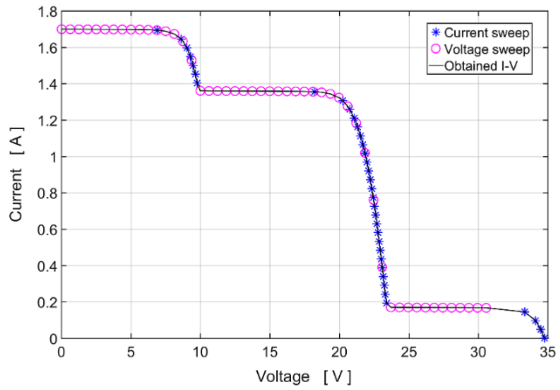

Figure 9: Results from a hybrid I-V sweep simulation.

The simulations show that it is it is possible to obtain satisfactory resolution in all parts of the I-V curve even with a modest number of points. In fact, the small gap seen near the lowest knee was due to not covering the entire voltage range in the voltage sweep all the way to the $\mathbf{V_{OC}}$. Fine estimation of the MPP is then possible by fitting locally the I-V curve in the vicinity of the 'blind' MPP (the measured MPP). Same applies to the $\mathbf{V_{OC}}$ and $\mathbf{I_{SC}}$.

From practical experience, the dynamic behavior of the electronic load used to sweep the I-V curve are of big importance. It may have a very fast response in constant current regulation mode but be very slow in constant voltage mode, thus making the hybrid sweeping too long.

Furthermore, some loads as the one used to obtain the results in Figs. 6 and 7 can have a 'jumpy' behavior due to saturation at either the open-circuit or short-circuit end. These I-V curves took 0.1 s to sweep. The observed behavior is clearly due to the load and not to the tested low-capacitance c-Si minimodule. Such load-related issues can be tackled by programing more sophisticated control waveforms, e.g. longer time steps near the saturation point(s). Any remaining outliers can be post-processed by using fitting techniques that discard them.

5 CONCLUSIONS

The results in the present work indicate significant accuracy improvements in the electrical characterization of PV modules. Specifically, a major reduction of the points number per I-V curve can be achieved. Dynamic point setting is not necessary which saves time and computational effort. Equidistant points suffice for the case of hybrid sweeping. More accurate determination of the shunt and series resistances ($\mathbf{R_P}$ and $\mathbf{R_S}$, respectively) is possible. And finally, the load's response time and resolution may not be superior thus preventing high equipment costs. We compared the presented methods in practical terms and implemented the variable current step sweeping in outdoor testing experiments. The proposed methodology achieves improved measurement accuracy and reduced data storage costs.

ACKNOWLEDGEMENTS

This project receives the support of the European Union, the European Regional Development Fund ERDF, Flanders Innovation & Entrepreneurship and the Province of Limburg. Our colleagues Willem Bertels, Wout Parys, and Patricia Elsen from KU Leuven's Civil Engineering department deserve our special thanks for installing the tested PV modules.

REFERENCES

[1] H. Goverde, D. Goossens, J. Govaerts, F. Catthoor, K. Baert, J. Poortmans and J. Driesen, "Spatial and Temporal analysis of wind effects on PV modules: Consequences for electrical power evaluation", Solar Energy, vol. 147, pp. 292-299, 2017.

[2] E. E. Van Dyk, A. R. Gxasheka and E. L. Meyer, "Monitoring current-voltage characteristics and energy output of silicon PV modules," Renewable Energy, vol. 30, pp. 399-411, 2005.

[3] F. Recart, M. Mäckel, A. Cuevas and R. Sinton, "Simple data acquisition of the current-voltage and illumination-voltage curves of solar cells," in IEEE WCPEC, 2006.

[4] M. M. Mahmood, "Transient analysis of a PV power generator charging a capacitor for measurement of the I-V characteristics," Renewable Energy, vol. 31, pp. 2198-2206, 2006.

[5] Y. Kuai and Y. S, "An electronic load for testing photovoltaic panels," Journal of Power Sources, vol. 154, pp. 308-313, 2006.

[6] N. Forero, J. Hernandez and G. Gordillo, "Development of a monitoring system for a PV solar plant," Energy Conversion and Management, vol. 47, pp. 2329-2336, 2006.

[7] J. Salmon and R. Phelps, "Solar cell measurement system for NPS Spacecraft Architecture and Technology Demonstration Satellite NPSAT1," in 17th Annual AIAAlUSU Conference on Small Satellites, 2003.

[8] M. G. Gunvench and C. Gurcan, "Solar simulator and I-V measurement system for large area solar cell testing," in Proceedings of the 2004 American Society for Engineering Education Annual Conference & Exposition, 2004.

[9] J. Fernandez-Reche and I. Canadas, "PSA Solar furnace, A facility for testing PV cells under concentrated solar radiation," Solar Energy Materials & Solar Cells, vol. 90, pp. 2480-2488, 2006.

[10] E. Duran, J. Galan, M. Sidrach-de-Cadrona and J. M. Andujar, "A new Application of the Buck-Boost-Derived Converters to obtain the I-V curve of PV Modules," in 38th IEEE PESC, 2007.

[11] E. Duran, M. B. Ferrera, J. M. Andujar and M. S. Mesa, "I–V and P-V curves measuring system for PV modules based on DC-DC converters and portable graphical environment," in Industrial Electronics (ISIE), 2010 IEEE International Symposium on, 2010.

[12] M. Bliss, T. R. Betts, R. Gottschalg and D. Infield, "Improved outdoor monitoring of photovoltaic modules," Proc. PVSAT-2, 2005.

[13] G. Van den Broeck, W. Parys, H. Goverde, J. Poortmans, J. Driesen, K. Baert and D. Saelens, "Experimental Analysis of the Performance of Facade-Integrated BIPV in Different Configurations," in 32nd European Photovoltaic Solar Energy Conference and Exhibition, Munich, 2016.

[14] G. Van den Broeck, B. Herteleer, H. Goverde, F. Catthoor, K. Baert and J. Driesen, "Substring-level Energy-yield Assessment of Photovoltaic Modules subject to Partial Shading Conditions," in European PV Solar Energy Conference and Exhibition, Hamburg, 2015.

[15] W. Parys, G. Van den Broeck, H. Goverde, K. Baert, D. Saelens, "Whole building energy analysis of a BIPV curtain wall." Advanced Building Skins, edition 11, Bern, 2016.

[16] G.H. Yordanov, "The PVGIS relative efficiency model: Equations for k_1 through k_6." Proceedings 29th EU PVSEC, 2014, Amsterdam, pp. 3297–3301.